

Water Vapor-Sodium Montmorillonite Interaction

G. L. RODERICK, Assistant Professor of Civil Engineering, University of Rhode Island; and

TURGUT DEMIREL, Associate Professor of Civil Engineering, Iowa State University

The interaction of water vapor with sodium montmorillonite was investigated with X-ray diffraction and sorption isotherm (gravimetric method) experiments. Expansion of the montmorillonite occurs in three increments. The data suggest that interlayer water builds up in a laminar fashion. The hysteresis of sorption isotherms is apparently due to the formation of a thixotropic structure and to attractive interlayer forces. BET parameters from adsorption isotherm data reflect adsorption only on external surfaces. Free energy data, computed from adsorption isotherm data and X-ray data, allow separation of the free energy change on adsorption into two components: one for adsorption on external surfaces, and one for adsorption on, and separation of, internal surfaces. The data also permit the estimation of swelling pressures exerted by sodium montmorillonite due to the uptake of interlayer water from the vapor phase.

•CLAY-WATER systems are of prime importance in the engineering use of soils; for example, in the prediction of bearing capacity, skin friction on piles, or settlement. Past research on these matters has emphasized mechanical aspects of soil-water systems. It has been recognized, however, that some problems such as secondary consolidation, swelling pressures, and cohesion are not solvable by a mechanistic approach. Therefore, it appears that a more fundamental knowledge of the clay-water system is essential for understanding and predicting the soil-mechanics behavior of clays.

The objectives of this study were to obtain some fundamental knowledge of the sodium montmorillonite water system from successive adsorption-desorption isotherms of water vapor on the montmorillonite, and from X-ray diffraction data obtained during adsorption and desorption.

EXPERIMENTAL PROGRAM

Material

Sodium montmorillonite was chosen as the material for this investigation because the expansive clays are the most troublesome in soil engineering practice. Also, this choice provided the opportunity to study the phenomenon of interlay adsorption of water.

The homoionic sodium montmorillonite sample was prepared from a commercially available Wyoming bentonite, Volclay-SPV, produced by ion exchange (1, 2).

Methods of Investigation

Sorption Isotherm Study.—Sorption isotherms of water vapor on sodium montmorillonite were determined by gravimetric method (3). Figure 1 shows the adsorption apparatus. Bulb A was the permanent water reservoir vapor source. B was a simple

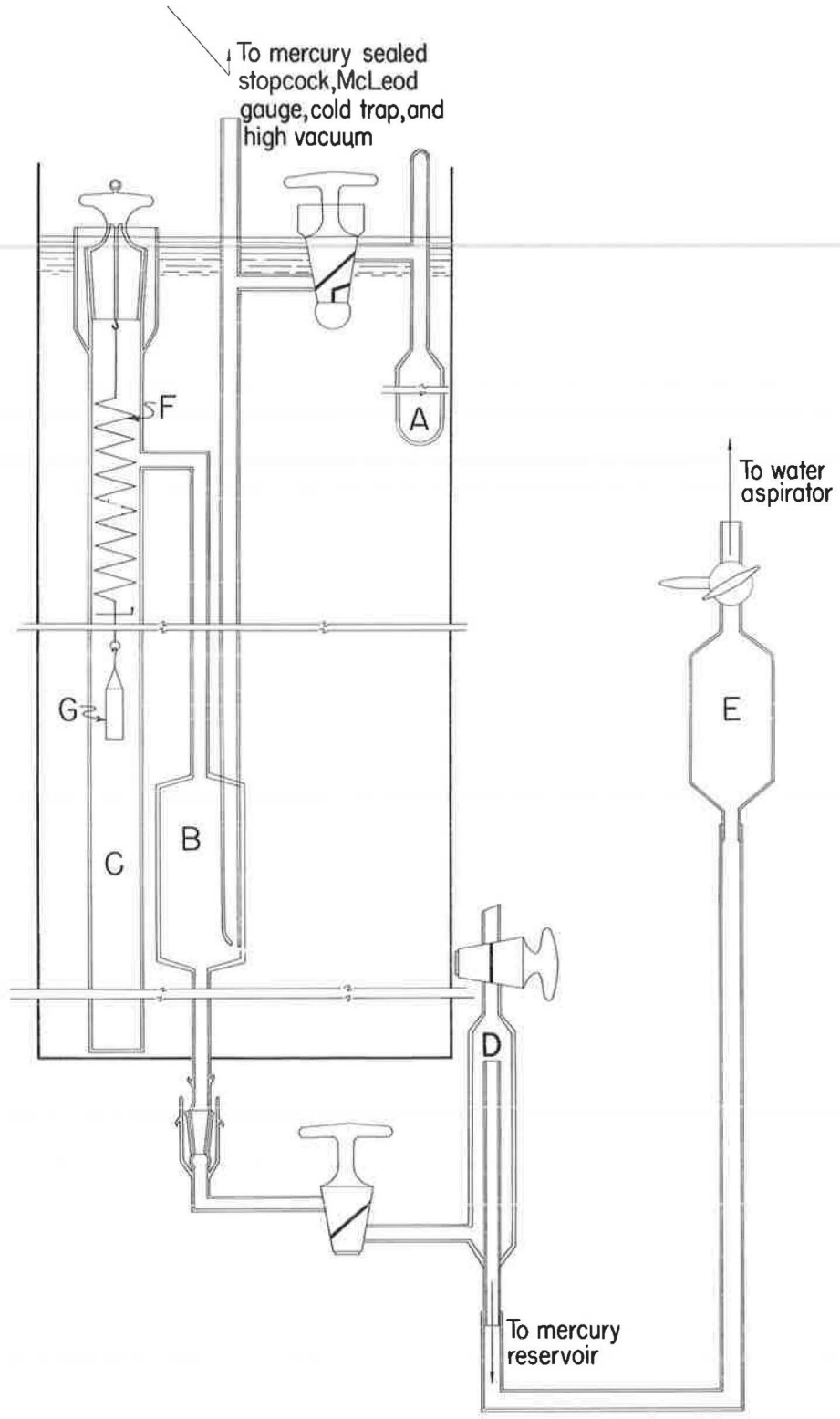


Figure 1. Adsorption apparatus.

mercury manostat-manometer combination for transferring vapor into the adsorption chamber, C, and for measuring vapor pressures. Mercury in B could be raised or lowered through air trap D into the mercury reservoir E. All glass parts were pyrex; all stopcocks were mercury-sealed, and high-vacuum silicone grease was used at all joints. A McBain-Bakr quartz spring balance, F, was suspended into the adsorption chamber from a mercury-sealed ground glass stopper, and a thin walled glass tubing sample holder, G, was suspended from the balance hangdown loop. The water reservoir, manostat-manometer, and adsorption chamber were immersed in a water thermostat maintained at 24.4 C. The apparatus was connected to a high-vacuum system by means of a mercury-sealed stopcock.

The sodium montmorillonite sample, in the sample holder, was dried for several weeks in an evacuated desiccator containing phosphorous pentoxide. The initial sample weight was 158.7 mg with a certified analytical balance. The sample was then placed in the adsorption chamber which, after a brief evacuation, was closed off by the manostat while the triple-distilled water in the reservoir was degassed by a repeated freezing-pumping-thawing process. With the reservoir closed off from the system, the adsorption chamber and sample were degassed by pumping at 10^{-5} mm Hg for several days. The manostat was then closed, the vacuum system closed off, and the water reservoir opened to allow water vapor into the right side of the system.

After thermal equilibrium at 24.4 C was attained, an initial pressure reading, p_0 , was taken with a cathetometer reading to 0.02 mm, and corrected for temperature, gravity, and meniscus. An initial balance reading was made with an optical reader; one division on the reader corresponded to 0.0239 mg of mass increase of the sample. A small increment of vapor was then transferred to the chamber through the manostat arrangement. A period of 24 hr was sufficient for the system to attain equilibrium. After this period the pressure difference on the manometer and the spring balance extension were measured. The equilibrium pressure, p , in the chamber was found by making the required corrections on the pressure difference observed and subtracting it from the saturation pressure, p_0 . The balance extension was converted to mass increase and divided by the initial sample weight to give the mass of vapor, q , adsorbed by one gram of montmorillonite. More and more vapor was transferred in the same manner until saturation pressure was attained.

In the vicinity of saturation an additional technique was used. After the vapor transfer, a small amount of condensation was formed in the chamber side of the manometer by cooling with a few cubic centimeters of cool water. Before saturation this condensation disappeared rapidly. At saturation the time for disappearance increased to several minutes. The mass of vapor adsorbed just before and at saturation differed by less than 0.1 percent.

The desorption isotherm was obtained by condensing more and more vapor back into the water reservoir by cooling it with water. The sample was pumped at relative pressures, p/p_0 , below 0.3.

The adsorption apparatus, optical reader and cathetometer were all securely mounted on a rigid steel frame tied to a heavy soapstone table top to prevent differential movements. The experimental error in determining p/p_0 was calculated to be ± 0.003 for all pressure ranges. The experimental error in determining q was $\pm 3 \times 10^{-5}$ gm/gm at low pressures and $\pm 3 \times 10^{-4}$ gm/gm near saturation pressure.

X-ray Diffraction Study.—The apparatus used in the X-ray study consisted of a Rigaku-Denki controlled atmosphere high-temperature X-ray diffractometer attachment converted to serve as an adsorption chamber. The furnace and its support base were removed, and a stainless steel sample holder (Fig. 2) was constructed to take their place. This sample holder could be aligned by using the translation, rotation, and inclination controls provided for alignment of the furnace. The arrangement of the water reservoir source for vapor, the manometer for pressure readings, the mercury-sealed stopcock connection between the reservoir and adsorption chamber, and the X-ray windows are shown in Figure 3. The stopcock was fastened securely to a small brass cylinder which was in turn attached to a larger cylinder which fit snugly over the top of the adsorption chamber. A glass tube was attached to the exhaust port coupling by a kovar metal tube and supplied the connection between the adsorption chamber and the portable vacuum system.

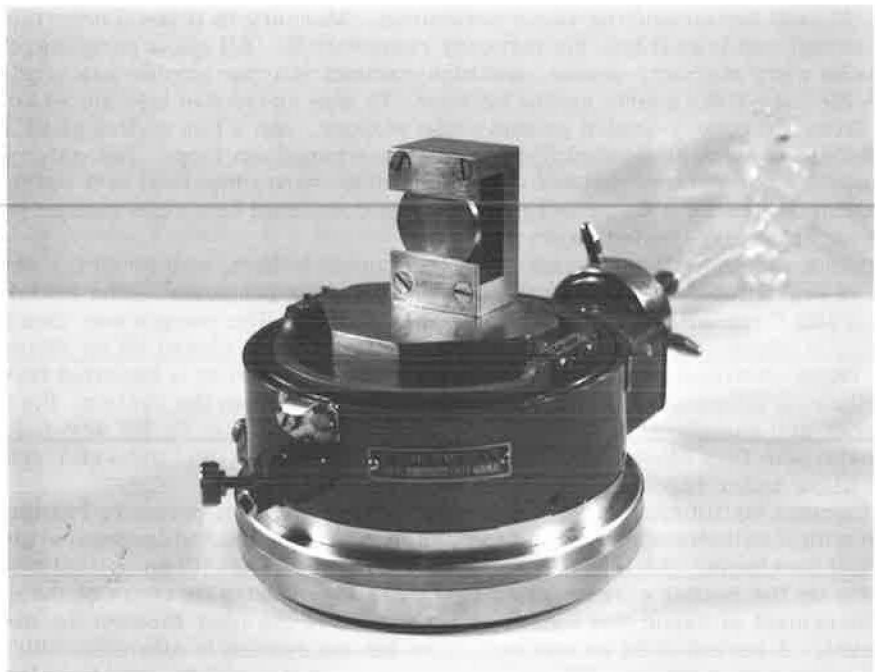


Figure 2. Sample holder for X-ray diffraction study.

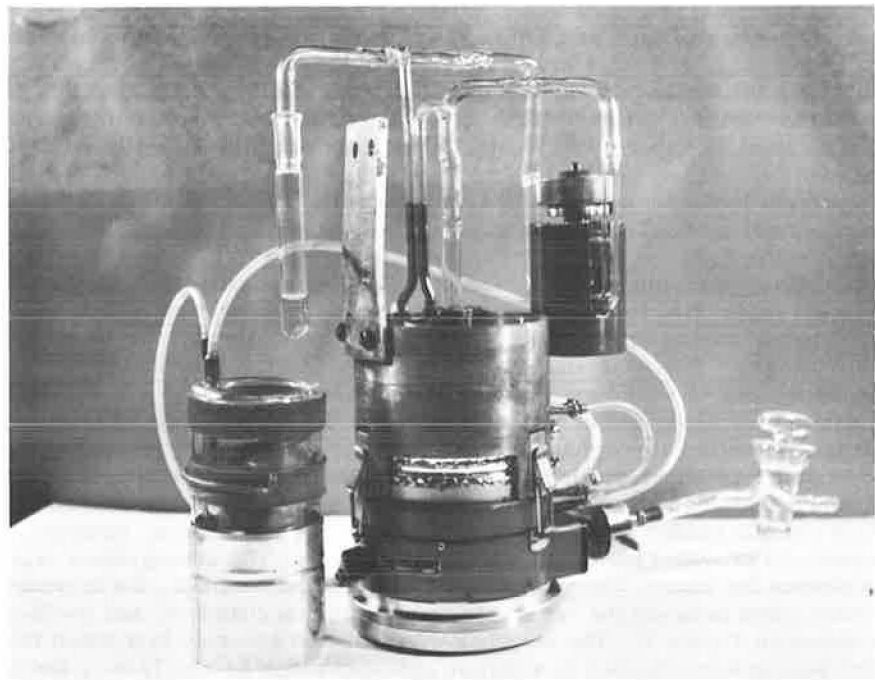


Figure 3. Apparatus for X-ray diffraction study.

The X-ray windows were made of 0.02-mm aluminum foil backed by a $\frac{1}{2}$ mil Mylar polyester film. If the aluminum foil alone was used, pinhole leaks developed in the windows during the experiment.

The adsorption chamber temperature was controlled by circulating water at constant temperature through the cooling tubes provided in the top and bottom portions of the apparatus. The constant temperature water was also circulated through a cooling coil fastened in a water filled dewar flask so that, when in position, the coil surrounded the water reservoir. In Figure 3 the flask is to the left of the apparatus. The constant temperature water source was thermostatically maintained at 22.99 C. The measured temperature in the dewar flask enclosing the water reservoir was 23.2 C during all readings.

A suspension of the sodium montmorillonite was pulled, by a water aspirator, through a 30-mm diameter medium-porosity fritted glass disc so that a thin layer of the clay was deposited on the disc. The sample was dried in an evacuated desiccator containing phosphorous pentoxide. It was then placed in the sample holder and the top cover of the apparatus was positioned. The triple-distilled water in the reservoir was degassed by a repeated freezing-pumping-thawing process. The stopcock was kept closed while the sample was pumped for several days to 10^{-4} mm Hg. The connection between the adsorption chamber and the vacuum train was cut and sealed; the apparatus was connected to the constant temperature water circulation system, placed on the XRD-5 diffractometer and the sample aligned. When thermal equilibrium was attained, the sample was X-rayed with copper $K\alpha$ radiation and five traces of the initial 9.82 Å 001 peak obtained. A manometer reading was taken, with a micrometer slide cathetometer reading directly to 0.001 mm, and corrected for temperature, gravity, and meniscus.

After obtaining initial peak and pressure readings, the stopcock was partially opened to allow a small increment of water vapor into the chamber. After a period of 24 hr the pressure difference and the new peak position were observed. Each new peak position was recorded five times. In this manner more and more water vapor was transferred to the chamber until the saturation pressure was reached. Desorption was accomplished by condensing vapor back into the water reservoir by cooling it with ice water until a p/p_0 of 0.3 was reached, and by freezing with a dry ice-acetone mixture to a p/p_0 of 0.03. The vacuum system was used to pump out the last increment.

The experimental error in determining p/p_0 was calculated to range from ± 0.007 at low pressures to ± 0.003 near saturation.

RESULTS

X-Ray Diffraction Study

The first order basal spacings and the widths of the observed diffraction peaks obtained for two cycles of adsorption-desorption of water vapor on sodium montmorillonite are plotted against the relative pressure at which they were observed in Figure 4. The points plotted are the average of five observations for each determination. The accuracy with which individual observations could be made depended on the size of the diffraction angle and on the sharpness of the peaks obtained, which varied with the relative pressure. The average variation from the average value for five observations of the basal spacing were less than ± 0.10 Å, with a maximum variation of ± 0.25 Å at small angles; for line widths the variations were from ± 0.01 to ± 0.10 degrees. The line widths of the diffraction peaks obtained were taken as the peak width at half-maximum intensity (4).

A shift of the adsorption curve for the second cycle from the position of that for the first is shown in Figure 4. The same behavior was observed with an earlier sample used in incomplete runs. The first adsorption curve followed the present one very closely up to a p/p_0 of 0.70, when a leak developed in the X-ray window. Another incomplete run with the same sample showed a shift to a position between those shown in Figure 4, somewhat closer to the curve for the second run. After solving the leakage problem, a new sample, from which the present data were obtained, was placed in the apparatus.

build up on each other by being hydrogen-bonded to the previous one. Taking 2.76 Å as the thickness of a water molecule (16, p. 464), their hypothesis results in a laminated stacking, causing a separation of 2.76 Å for each molecular layer of water.

Macey (17) noted the lattice similarities between the basal planes of ice and of clay minerals. He suggested that the ice structure develops on clay mineral surfaces with the hexagonal molecular configuration of the basal plane of ice. This structure tends to build outward from the surface. Forslind (18) suggested the same ice structure postulated by Macey, but based his argument on the Edelman-Favejee structure rather than the Hofmann-Endell-Wilm structure of montmorillonite.

Demirel (1) presented two ways in which the ice structure may develop in the interlayer regions. Using data reported in the literature and his own data for various species of homoionic montmorillonites, he found evidence to support the buildup of an ice structure in which the first hexagonal network is shared by two montmorillonite platelets, causing a separation of 2.76 Å; two hexagonal networks are stacked and held by the two silica surfaces, causing a separation of 5.52 Å; the third and fourth molecular layers of water fill in between the hexagonal networks forming tetrahedrons with the water molecules of the network. A complete unit cell of ice is formed with the entrance of the fourth molecular layer of water, causing a separation of 7.36 Å. The fifth and sixth layers of water enter between the unit cell of ice and the clay surfaces, forming hexagonal networks and causing separations of 10.12 and 12.88 Å, respectively.

Barshad (19) suggested an arrangement which becomes progressively denser with the addition of water. He postulated arrangements for water molecules that would give various increases in basal spacing for each additional molecular layer of water, depending on the position of water molecules with respect to the basal oxygens of the clay surface and to water molecules of previously adsorbed layers. The first layer would give spacing increases of 2.76 or 1.78 Å; other layers would give increases of 2.76 or 2.09 Å.

The continuity of the basal spacing vs relative pressure curve of the present study has been attributed to the simultaneous existence of clay platelets separated by various molecular layers of water. If all of the interlayer water is removed at zero relative pressure, a sharp peak is observed corresponding to the collapsed basal spacing of sodium montmorillonite, about 9.60 Å (20). As the relative pressure increases, some water begins to penetrate between some of the clay layers. If it is assumed that at low relative pressures the system consists primarily of layer spacings corresponding to zero and one molecular layers of water between platelets, i. e., that the contributions of layers separated by 2, 3 or more molecular layers of water to the observed diffraction peaks are negligible, then the system may be treated as a random interstratification of two components. At somewhat higher relative pressures the observed peaks may be treated as composite peaks from another random two-component system, one component corresponding to one molecular layer of interlayer water and the other to two layers. This may be extended to higher increments of expansion. As the relative pressure increases, the relative proportions of the two components change and the observed diffraction peaks migrate from the position of the first pure component, A, toward that of the other pure component, B. According to MacEwan, Amil and Brown (7), in a preliminary analysis there will be no great error in assuming that the peaks move linearly between the two pure component positions. When the distances from the observed peak to the A and B positions are x and y , respectively, the proportion of component A is deduced to be $y/(x + y)$. As the observed peak migrates from the A position, it first becomes diffuse and then sharper again as it approaches the B position. Taking the line width to be a function of the nonconstancy of layer separations, we would suspect that a maximum width would correspond to the most random distribution of the two layer separations, and that this would occur when the relative proportions of the two components are nearly equal. Although this conclusion may not be strictly true (7), it is felt that assuming the maximum line width corresponds to an A/B ratio of one will be in no greater error than that in assuming the peak migration to be linear.

If it is assumed that (a) the system of the present study may be treated as a random interstratification of two components; (b) peak migration between pure component positions is linear; and (c) maximum line widths occur when the relative proportions of the

TABLE 1
CALCULATED FIRST ORDER BASAL SPACINGS OF
SODIUM MONTMORILLONITE

No. of Molecular Layers of Water	Laminated, Stacking Ar- rangement of water		Ice-like Arrangements of Water Molecules	
	Calculated Basal Spacings (Å)	Avg., Two Successive Spacings (Å)	Calculated Basal Spacings (Å)	Avg., Two Successive Spacings (Å)
0	9.60		9.60	
1	12.39	10.98	12.36	10.98
2	15.12	13.74	15.12	13.74
3	17.88	16.50	15.12	13.74
4	20.64	19.26	16.96	16.04
5	23.40	22.02	19.72	18.34

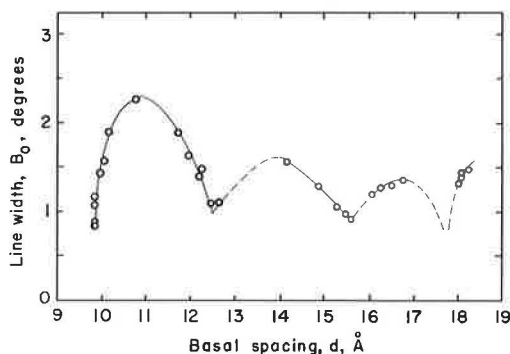


Figure 6. Variation of line widths with basal spacings of sodium montmorillonite.

two components are equal, the line width and basal spacings data of this study may be used to test possible arrangements for the interlayer water that have been postulated by others. The minimum line widths should correspond to a basal spacing near that calculated from the proposed arrangement for an integral number of molecular layers of water between clay platelets. If assumptions (b) and (c) hold, the maximum line widths should occur at a basal spacing which is the average of those calculated for two successive layers of water between platelets.

The observed basal spacing and line widths for the first adsorption run are plotted against one another in Figure 6.

Using 9.60 Å as the collapsed basal spacing of sodium montmorillonite, the basal spacings for integral numbers of molecular layers of water between platelets and the averages of each two successive spacings were calculated for the various postulated interlayer water arrangements. At low pressures, the values obtained for the laminated structures and the ice-like structure of Demirel (1) showed the best agreement with experimental data; the values calculated for these arrangements are given in Table 1. The first maximum line width occurs at a basal spacing of about 11.0 Å, very near the 10.98 Å average calculated for zero and one molecular layers of water. The first minimum line width occurs at about 12.5 Å, which is close to the calculated value of 12.36 Å for one molecular layer of water. Although the observed data are scarce, the second maximum line width appears to be about 14 Å, which is reasonably near the 13.74 Å average for one and two layers of water. The second minimum line width is at about 15.5 Å, somewhat higher than the 15.12 Å calculated for two layers of water. The higher than expected basal spacings corresponding to the observed line width minima may be due to failure of the assumption of a two-component system in the region near the peak position for a pure component (all platelets at one spacing). As the peak position approaches that for a pure component, the number of platelets at the next increment of expansion increases, and probably their contributions to the observed peak are no longer negligible. Therefore, the system in

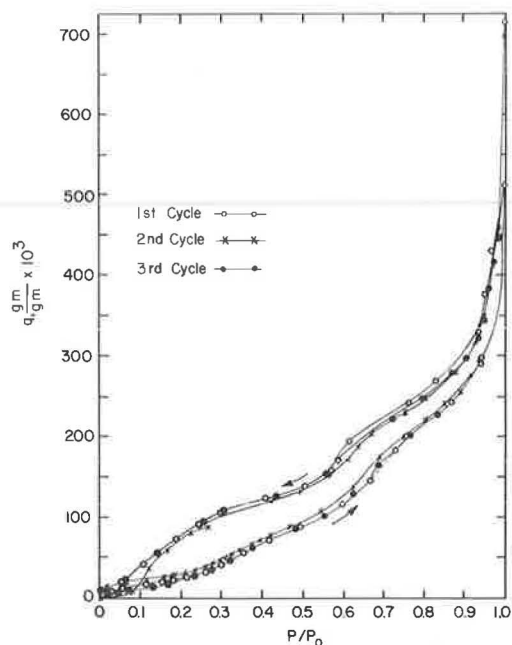


Figure 7. Adsorption and desorption isotherms of sodium montmorillonite.

The data give evidence of the formation of a laminated arrangement of the interlayer water rather than an ice structure for sodium montmorillonite with up to three layers of water. The arrangement in individual layers of water cannot be ascertained from these data. More detailed studies with sodium montmorillonite, and with other materials such as calcium montmorillonite, may give more complete evidence. Also, better data on the intensity of diffraction peaks may be helpful. Other methods of investigation, such as nuclear magnetic resonance studies and heat capacity studies, may permit more definite conclusions to be drawn.

Sorption Isotherm Study

Figure 7 is a plot of the sorption isotherms for three successive adsorption-desorption cycles. The adsorption and desorption branches fall in different regions of the plot, illustrating the hysteresis expected with porous absorbents (3).

The data of the present study show that the adsorption branch is more closely reproduced on successive runs than the desorption branch. After a p/p_0 value of about 0.28, the adsorption curves for the first and third cycles follow each other very closely, within the experimental error previously given. The desorption curves for these two cycles are not in as good agreement until relative pressures below 0.30 are reached. Neither the adsorption nor desorption branches for the second run, which began at a higher value of q , agree very well with those for the other cycles. If the isotherm for the second cycle is started at the origin, the agreement is much better for adsorption than for desorption. The data suggest that the adsorption branch may be the true equilibrium curve. This would be in agreement with the "ink bottle" theory of McBain (21) and the "open pore" theory of Foster (22), both of which explain the hysteresis on the basis of the shape and arrangement of the pores in which capillary condensation takes place.

Barrer and MacLeod (23) studied the adsorption of various nonpolar and polar gases and vapors, including water vapor, by a sodium-rich montmorillonite, and gave an

this region is likely to be one of three rather than two components and the observed minimum line width may well occur at a slightly higher average basal spacing.

The rest of the data (Fig. 6) are not very conclusive. The X-ray data in this region are all in the p/p_0 range of 0.97 to 1.00, and are quite crowded. However, Figure 6 does show that a probable maximum line width does occur at a basal spacing greater than about 16.7 Å. This is closer to the 16.5 Å average calculated for laminated structures than it is to the 16.04 Å average for the ice structure. The last group of points (Fig. 6) suggests that a minimum line width may occur at an average basal spacing of slightly less than 18 Å. Again, this is nearer the 17.88 Å calculated for three molecular layers of water in a laminated structure than it is to the 16.96 Å calculated for four molecular layers of water in an ice structure. More extensive data at high relative pressures are needed to draw a definite conclusion. Smaller increments of vapor transfer at high relative pressures may enhance the line width-basal spacing relationship in this region.

explanation for the hysteresis observed when polar vapors are adsorbed in the interlayer regions. When nucleation of an adsorbate-rich phase occurs around the periphery of crystallites, it must be associated with strain and interfacial free energies, which slow down the free development of the adsorbate-rich phase until the pressure has exceeded the value for true thermodynamic equilibrium between the vapor and separated montmorillonite layers with and without interlayer adsorbate. On desorption, the development of the adsorbate-poor phase in the interlayer region is delayed by strain and interfacial free energy until the pressure has fallen below that for true equilibrium, and a hysteresis loop is observed.

Hirst (24) also developed a similar explanation for hysteresis, associated with interlayer adsorption. Attractive forces between layers prevent penetration of the adsorbate until a threshold pressure is reached. These forces are then overcome by forces leading to penetration, and the layers separate to admit a layer of adsorbate. On desorption, the layers are initially separated and their attractive interaction weakened, whereas the forces tending to separate them are high. The layers cannot come together until the amount of interlayer adsorbate, and thus swelling pressure, are substantially reduced. Therefore, a hysteresis loop is observed.

According to Brunauer (3, p. 409) the adsorption process probably causes a change in the pore volume which may be either reversible or irreversible. This may result in different pore arrangements in the external surfaces of the montmorillonite, and may account for the difference in the adsorption curves prior to a relative pressure of about 0.28 for the first and third cycles. X-ray diffraction data show that at a p/p_0 of about 0.28 the basal spacing begins to increase rapidly with increasing p/p_0 . In this region the adsorption curves begin their agreement, suggesting that the effect of the interlayer surfaces far outweighs that of the external surfaces.

The general shape of the adsorption and desorption isotherms (Fig. 7) is very similar to those presented elsewhere (1, 13, 23, 25). Figure 4 shows that the steeper portion between p/p_0 of 0.25 and 0.45 in Figure 7 corresponds to the first increment of layer separation. The steeper portion of the isotherm, beginning at a p/p_0 of 0.65, corresponds to the second increment of layer separation. The argument proposed by Barrer and MacLeod explains the form of the adsorption isotherm of this study. The initial water adsorbed is mainly confined to the external surfaces of the clay. After an approximate threshold pressure is reached, the water molecules penetrate more freely between clay sheets, and cause separation. With water vapor, a second stage of interlayer adsorption occurs and is reflected by the second steeper portion of the isotherm. As p/p_0 approaches 1.0, capillary condensation occurs. The X-ray data show that a third increment of layer separation also occurs at high relative pressures.

The desorption isotherms show a pronounced dip in the relative pressure range of 0.65 to 0.30. This is also shown in data of others (13, 23, 25). Barrer and MacLeod attribute the steep portion of this dip to the removal of interlayer adsorbate; this process occurs at an approximate threshold pressure below that for the adsorption curve. X-ray data of the present study show that the basal spacing remains nearly constant at 16 Å in the relative pressure range 0.65 to 0.50, corresponding to the steep portion of the dip. This would indicate that the greater portion of the water being desorbed is from the external surfaces.

Barrer and MacLeod (23) observed hysteresis loops for the adsorption-desorption of nonpolar gases and vapors on their montmorillonite. Since these adsorbates were adsorbed only on external surfaces, the reasons given for hysteresis with polar adsorbates are not applicable. They suggest that when the clay is lubricated by a film of capillary condensate some of the clay particles are drawn by surface tension forces into a thixotropic structure. This more regular array then retains capillary condensed adsorbate more firmly than would a purely random array. When the film of condensate becomes sufficiently dilute it ceases to lubricate and hold the thixotropic structure together. The array then becomes more random again, and must give up the remaining condensate. The desorption isotherm becomes steeper and, with nonpolar adsorbates, closes the hysteresis loop.

In view of the X-ray data of the present study, it is proposed that the foregoing argument may be applied to the desorption of water vapor in the relative pressure range

of 0.65 to 0.50. The steep portion of the isotherm in this range is, therefore, due to the destruction of a thixotropic structure with its accompanying release of capillary condensed water. The X-ray data show that removal of the last layer of interlayer water corresponds to a steep portion of the desorption isotherm beginning at a p/p_0 of about 0.30. The hysteresis explanations of Hirst (24) and of Barrer and MacLeod (23) are applicable in this region.

Figure 7 shows that the desorption branches for the first and third cycles do not come back to the initial q value, but that the desorption branch of the second cycle does reach this value. A possible explanation for the more complete desorption for the second cycle is proposed. Figure 7 shows a break in the second desorption curve at a relative pressure of about 0.25. At this point no vapor transfers were made for a period of 18 days, after which it was observed that the sample had desorbed more water and the relative pressure had increased as shown by the shift (dashed line) to a position lower and to the right. Two more days disclosed no additional change. The next vapor transfer caused a shift down and to the left (second dashed line) in one day. Before the 18 days with no vapor transfers, it appeared that the second desorption curve was approaching the path followed in the first run and later followed in the third cycle. However, after the idle period the desorption curve became steeper and the zero value of q was attained with relative ease. On the third run, with no prolonged nonvapor-transfer period, a special effort was made to reach the initial value of q . Even with a final pumping period extending over a period of three weeks, the value of q could not be brought substantially lower than that attained on the first run. This suggests that the remaining water was trapped in external pores (such as McBain's ink bottle pores) and/or in the interlayer regions. X-ray diffraction data (Fig. 4) indicate that at a relative pressure of 0.25 the last layer of interlayer water had started to be withdrawn. This is also shown by the data of Mooney et al. (10) and of Gillery (11) reproduced in Figure 5. The prolonged period of no vapor transfer may allow for particle rearrangement and for escape of water from pores and interlayer regions which would be blocked off by contraction of the mass on further desorption.

The behavior previously discussed for a prolonged nonvapor-transfer period would indicate that equilibrium was not attained in the 24-hr period between vapor transfers, at least in that region of the desorption isotherm. There was a similar nonvapor-transfer period of 20 days, at a relative pressure of 0.70 on the desorption curve, with no significant change in the location of the position observed 24 hr after the vapor transfer, indicating equilibrium was attained in 24 hr.

No relaxation of the type described here was observed for adsorption runs; 24 hr were enough for attainment of equilibrium.

Application of BET Theory

In the low pressure region, the Brunauer, Emmett and Teller theory of multimolecular adsorption (26) predicts the adsorption equation will be

$$\frac{p}{q(p_0 - p)} = \frac{1}{q_m C} + \frac{C - 1}{q_m C} \frac{p}{p_0}$$

where q_m is the mass of vapor adsorbed when solid surface is covered by a monolayer, and C is a constant approximately equal to $e^{(E_1 - E_L)/RT}$, where E_1 is the heat of adsorption of the first layer and E_L is the heat of liquefaction of the vapor.

The values of the BET function, $\frac{p}{q(p_0 - p)}$, calculated from the sorption isotherm data, are plotted against p/p_0 for the three sorption cycles (Fig. 8). Generally, BET plots have a straight line region only between p/p_0 of 0.05 to about 0.3 (27, p. 481). A fairly straight line is obtained for the adsorption data between p/p_0 of 0.05 and 0.18. Comparison with the initial adsorption curve for basal spacings (Fig. 4) shows that at p/p_0 of 0.18 the first increment of interlayer separation is just beginning. Therefore,

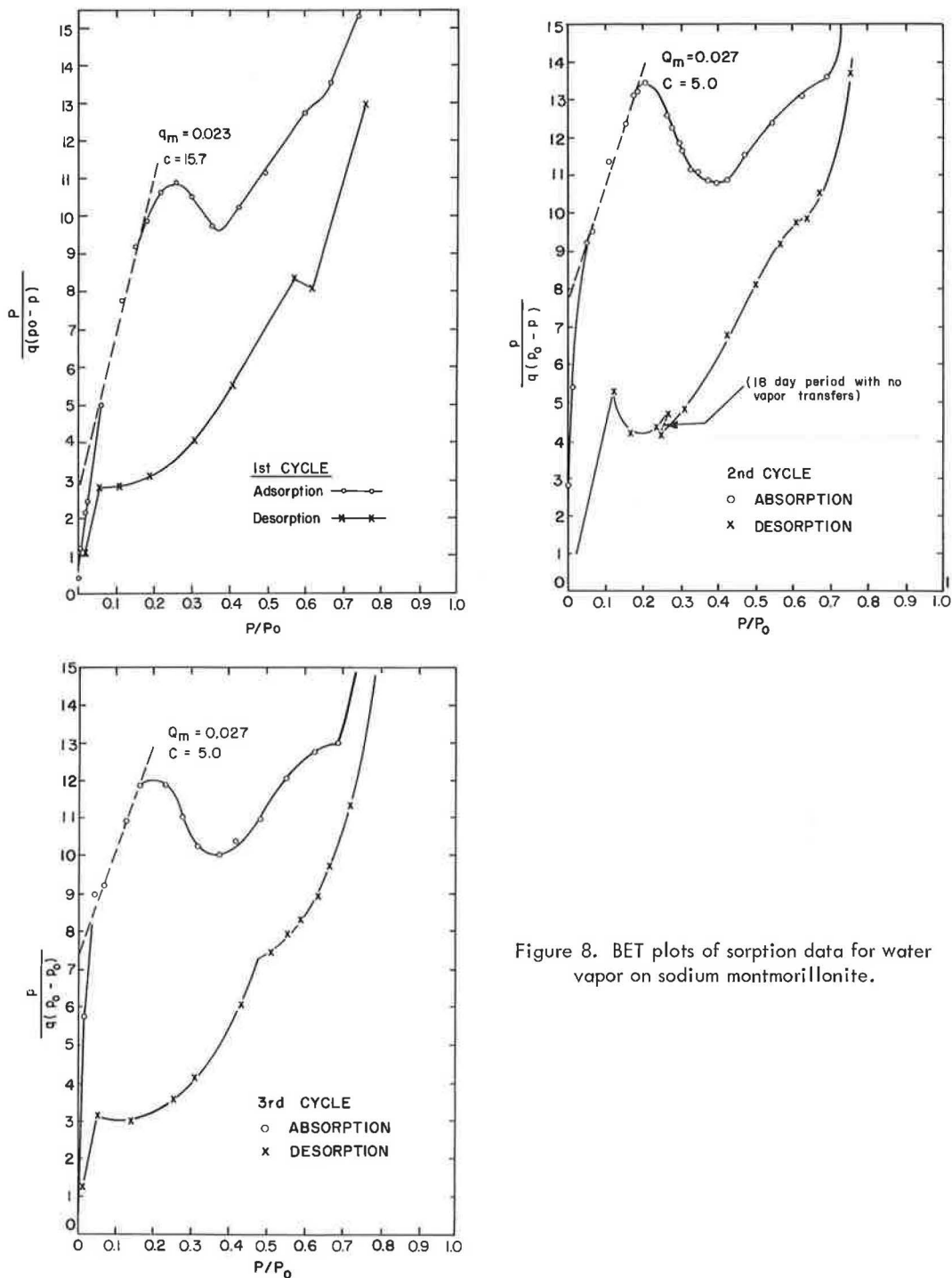


Figure 8. BET plots of sorption data for water vapor on sodium montmorillonite.

it was concluded the linear portion of the BET plot represents adsorption taking place predominantly on the external surfaces of the montmorillonite, and the BET parameters q_m and C represent the external surfaces (Fig. 8).

The present BET plots show a hump at a p/p_0 of about 0.2 and another deflection point at a p/p_0 of about 0.6 to 0.7. The X-ray data show that these values correspond with the initial portions of the first and second increments of expansion. Apparently this behavior is due to expansion making accessible surface areas not initially available for adsorption.

The pronounced hump at a p/p_0 of 0.20 appears to be a characteristic which occurs only with sodium Wyoming montmorillonite (Volclay). The adsorption data of Hendricks et al. (6) for sodium Wyoming montmorillonite (Volclay) yield a similar hump, whereas their data for sodium Mississippi and California montmorillonites do not. The data of Johansen and Dunning for sodium Wyoming montmorillonite (Volclay) would seem to be an exception; however, their data (25, Fig. 2) show no experimental observations in the p/p_0 range in which the hump occurs. Also, the q_m value of 0.056 obtained from their data is in very good agreement with values of 0.054, 0.058 and 0.055 obtained if the present BET plots in the p/p_0 range of 0.4 to 0.6 are extrapolated back to low pressures. Orchiston's data for sodium Arizona montmorillonite (28) show a high point on the BET plot at a p/p_0 of 0.05. This may represent a behavior similar to that observed more clearly with the present data (i.e., adsorption on external surfaces before penetration of water between clay layers) and may indicate that expansion begins at an appreciably lower relative pressure than for the Wyoming material.

External Surface Area.—If the area, s , of the adsorbent surface occupied by each water molecule of the monolayer is known, the parameter q_m could be used to determine the external surface area, A_e , per gram of montmorillonite by the expression:

$$A_e = \frac{Nq_ms}{M}$$

where N is Avogadro's constant, M is the molecular weight of the adsorbate, and q_m is expressed per gram of adsorbent. If the water molecules are in a closest packing arrangement, s is equal to 10.8 \AA^2 . However, other investigators have suggested other spatial geometric arrangements which result in other than closest packing for the monolayer coverage. The arrangement of Hendricks and Jefferson (5) gives an area of about 11.5 \AA^2 ; the basal plane of ice structures of Macey (17), Forslind (18) and Demirel (1) give an area of about 17.5 \AA^2 . External surface areas per gram of sodium montmorillonite, A_e , were computed using each of the foregoing areas for the water molecule and the q_m values obtained from the adsorption data (Table 2). The external area increased somewhat during the first adsorption-desorption cycle; the sorption process may result in different pore shapes and volumes in the external surfaces and in different arrangements of the surfaces, thus making more area available for adsorption. The external areas obtained are larger than those reported by others as determined from nitrogen adsorption, i.e., 41 to $71 \text{ m}^2/\text{gm}$ by Emmett et al. (29), $33 \text{ m}^2/\text{gm}$ by Mooney

TABLE 2
EXTERNAL SURFACE AREAS PER GRAM OF SODIUM
MONTMORILLONITE CALCULATED FROM WATER
VAPOR ADSORPTION DATA

Cross-Sectional Area per Water Molecule, \AA^2	External Surface Area, A_e (m^2/gm)		
	First Cycle $q_m = 0.023$	Second Cycle $q_m = 0.027$	Third Cycle $q_m = 0.028$
10.8	83.0	97.4	101.1
11.5	88.3	88.3	107.7
17.5	134.4	157.8	163.7

et al. (13), 38 m²/gm by Johansen and Dunning (25) and 24.5 m²/gm by Zettlemoyer et al. (30). This indicates some portions of the external surfaces are accessible to water vapor but not to nitrogen. Also, the line width data of Figure 4 show that there may be a small amount of water penetration into interlayer regions.

Heat of Adsorption.—The C parameters obtained in this study were used to calculate $E_1 - E_L$ values for the first monolayer of water adsorbed on external surfaces. The values, corrected according to Clappitt and German (31), were 3.3, 2.7 and 2.7 Kcal/mole and were in good agreement with values reported elsewhere (1, 28). Calculations from the calorimetric heat of immersion data of Zettlemoyer et al. (30) yielded $E_1 - E_L$ values of 3.0 to 3.7 Kcal/mole for the first monolayer on external surfaces.

The heat of adsorption curve presented by Zettlemoyer et al. (30, Fig. 4) from their heat of immersion and adsorption isotherm data does not show good agreement with isosteric heat of desorption isotherm data curve of Mooney et al. (13, Fig. 5) from desorption isotherm data. It does, however, show good agreement with the isosteric heat of adsorption data of Takizawa (32) from adsorption isotherms with Niigata bentonite. This may indicate that the adsorption isotherm is nearer the true equilibrium curve than the desorption isotherm.

Free Energy Changes

Free Energy of Wetting.—The free energy of wetting of sodium montmorillonite may be given as (1):

$$\Delta F = (\gamma_{sl} - \gamma_{so}) + \alpha \Delta V$$

where γ_{sl} is the solid-liquid interfacial tension, γ_{so} the surface tension of the solid in vacuum, α the interlayer surface area per cm² of total surface, and ΔV the free energy change per cm² of interlayer surface due to separation of layers against the force of interaction. To calculate ΔF from the adsorption isotherms, Bangham's free energy equation (33) was used; it can be expressed as:

$$-\frac{RT}{MA} \int_0^1 \frac{q}{p/p_0} d(p/p_0)$$

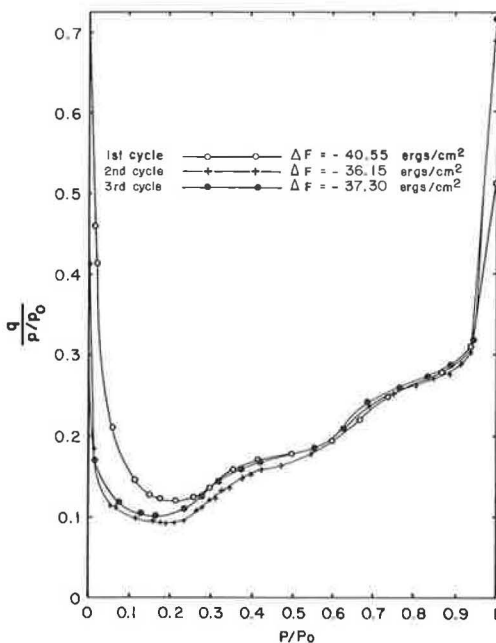


Figure 9. Plots for integration of Bangham's free energy equation for water vapor adsorption on sodium montmorillonite.

where R is the gas constant, T the absolute temperature, M the molecular weight of water, and A the specific surface of sodium montmorillonite. Figure 9 plots $q/(p/p_0)$ vs p/p_0 for graphical integration of the foregoing equation. From crystallographic data, A was determined to be 748 m²/gm for the sodium montmorillonite. The error in values of ΔF obtained was estimated to be about ± 6 percent. The free energies of wetting thus determined were -40.55 ± 2.43 , -36.15 ± 2.17 and -37.50 ± 2.24 ergs/cm² for the first, second and third adsorption runs. These values are in good agreement with that of -34.76 ± 1.91 ergs/cm² determined earlier for sodium montmorillonite (1).

Free Energy Changes on Adsorption.—Fu and Bartell (34), in their paper on the

surface areas of porous adsorbents, evaluated the integral

$$-\frac{RT}{M} \int_0^{p/p_0} \frac{q}{p/p_0} d(p/p_0)$$

at various values of p/p_0 for the adsorption of vapors on porous solids. When q is the mass of vapor adsorbed per gram of solid, the value obtained is the free energy change, $\Delta\Delta F$ in ergs/gm of solid, for adsorption from a relative pressure of zero to p/p_0 . When $\log (\Delta\Delta F)$ was plotted against $\log (p/p_0)$, two straight-line portions were obtained.

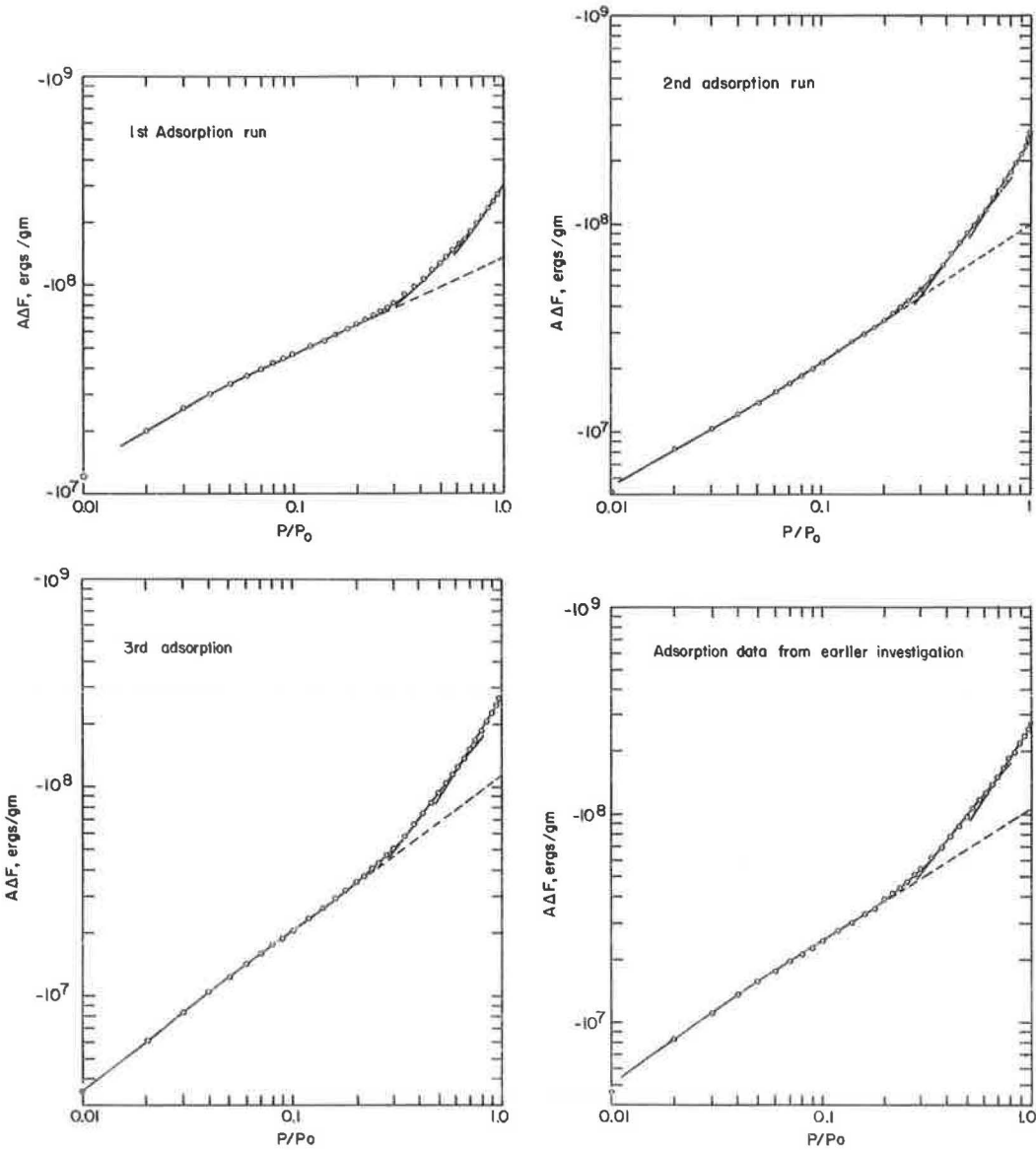


Figure 10. Log-log plots of free energy change vs relative pressure.

In discussing their method, Fu and Bartell state: "It is also conceivable that, with suitable interpretations, this method can be utilized to study the expansion or deformation of porous materials caused by the adsorption of various vapors." Sodium montmorillonite is a porous material which undergoes expansion with adsorption of water vapor; therefore, it was felt that an analysis similar to that of Fu and Bartell may be instructive. The values of the previously cited integral for increasing increments of p/p_0 , up to and including the saturation point, for the adsorption data of the present study were determined by graphical integration. This was also done with the adsorption data obtained earlier for sodium montmorillonite (1). Values of the integrals, $A\Delta F$, were thus obtained for four complete adsorption runs involving two separate samples of the material.

Plots of $\log(A\Delta F)$ vs $\log(p/p_0)$ are shown in Figure 10 for each run. Each of the plots displays three straightline portions (implying equations of the type $A\Delta F = \alpha(p/p_0)^\beta$ for various portions) rather than the two obtained by Fu and Bartell. The portions of the plots below p/p_0 of about 0.05 are not strictly linear, but show breaks in the slopes in the p/p_0 range of 0.045 to 0.055. This is in agreement with the observations of Fu and Bartell, who reported nonlinearity below p/p_0 of 0.05 and attributed it to the decreased accuracy in determining q values at very low pressures.

Comparison of Figure 10 with the X-ray data for the initial adsorption run reveals that the break in the $\log(A\Delta F)$ plot at a p/p_0 of 0.16 to 0.18 corresponds closely with the beginning of an increase in the basal spacing from 9.8 Å. The break at a p/p_0 of about 0.65 corresponds quite closely with the beginning of a second increment of expansion from a basal spacing of 12.5 Å; the break at a p/p_0 of 0.95 corresponds closely with the beginning of the third increment of expansion from a basal spacing of about 15.5 Å. The last two breaks also correspond very well with observed minima in the line width plot of Figure 4; these minimum line widths indicate the majority of the clay platelets have the basal spacing noted. On the basis of these correlations it was concluded that the portion of the $\log(A\Delta F)$ vs $\log(p/p_0)$ plot below p/p_0 of 0.16 to 0.18 reflects the energy changes due to adsorption on external surfaces only; at higher pressures energy changes due to adsorption on the internal surfaces are included and reflect the energy of interaction between clay platelets. The slope changes apparently reflect the differences in platelet interaction energies at increasing increments of expansion.

Fu and Bartell (34) attributed the change of slope in their plots to capillary condensation in the pores of the adsorbent. In the present system capillary condensation probably occurs in external pores in the higher relative pressure range, but its effect on the energy changes is apparently masked by those effects caused by adsorption on the internal surfaces. According to Barrer and MacLeod (23), capillary condensation of water between montmorillonite particles does not occur until the relative pressure approaches 1.0.

The relation between the free energy change and separation of clay platelets is shown in Figure 11. The values of $A\Delta F$ for the first adsorption run are plotted against platelet separation h , at the same p/p_0 , obtained from the X-ray diffraction data; $A\Delta F$ data for the other adsorption runs produce similar plots. Figure 11 shows sharp breaks corresponding closely with the slope changes in Figure 10. Also, the breaks occur when h values are very nearly integral multiples of 2.8 Å, the thickness of a water molecule. This gives additional evidence that the interlayer water builds up in a lamellar fashion.

Expansion Energies.—If the free energy changes could be divided into two components, one for adsorption on external surfaces and another for adsorption on internal surfaces, it would be possible to evaluate the expansion energies, i. e., the free energy change due to adsorption on, and separation of, the internal surfaces.

The free energy change brought about by the adsorption, on a solid surface, of a film at equilibrium with a vapor at some pressure, p , may be expressed as (27, p. 264)

$$\Delta F = \gamma_{sv} - \gamma_{so} \text{ ergs/cm}^2 \quad (1)$$

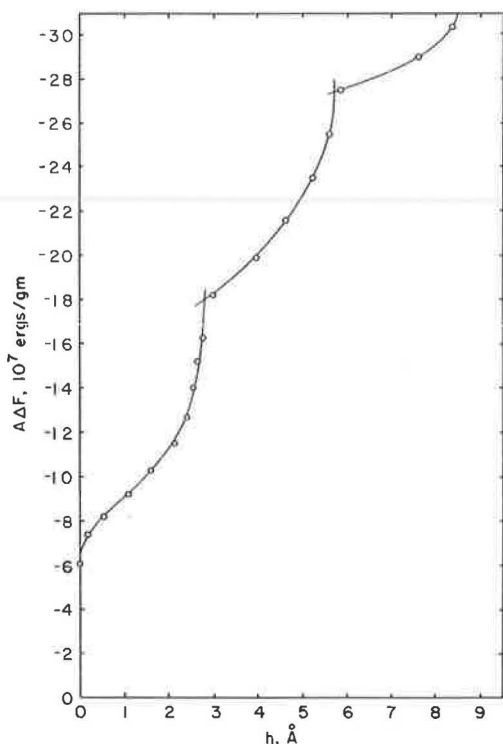


Figure 11. Plot of total free energy change vs interlayer separation, first adsorption run.

where γ_{so} is the surface free energy of the solid surface in vacuum, and γ_{sv} is that of the solid-vapor interface in equilibrium at pressure p . When the solid-vapor interface is in equilibrium with the saturated vapor, the free energy change is

$$\Delta F = \gamma_{sv0} - \gamma_{so} \text{ erg/cm}^2 \quad (2)$$

where γ_{sv0} is the surface free energy of the solid-vapor interface at the saturation pressure. According to Jura and Harkins (35), when the solid is wetted by the liquid, γ_{sv0} is equal to $(\gamma_{sl} + \gamma_{lv})$; γ_{sl} is the solid-liquid interfacial free energy and γ_{lv} is the surface free energy of the liquid in equilibrium with its own vapor. We have, therefore, at saturation

$$\Delta F = \gamma_{sl} - \gamma_{so} + \gamma_{lv} \text{ ergs/cm}^2 \quad (3)$$

If capillary condensation occurs, the γ_{lv} term drops out of Eq. 3. For the present system adsorption occurs only on the external surfaces of the clay at low relative pressures. Since only external areas, A_e , are involved, the free energy change is given by

$$A_e \Delta F = A_e (\gamma_{sv} - \gamma_{so}) \text{ ergs/gm} \quad (4)$$

If only the external areas were available for adsorption over the entire relative pressure range, it is proposed that the relationship $A_e \Delta F = \alpha(p/p_0)^\beta$ would continue to be obeyed. Under these circumstances, the linear portion of the $\log(A_e \Delta F)$ vs $\log(p/p_0)$ plot between p/p_0 of 0.05 to 0.18 would be extended to a p/p_0 of 1, as shown by the dashed lines (Fig. 10). The free energy change at saturation would be

$$A_e \Delta F = A_e (\gamma_{sl} - \gamma_{so} + \gamma_{lv}) \text{ ergs/gm} \quad (5)$$

If capillary condensation were to occur (still only external surfaces available), a behavior such as that observed by Fu and Bartell (34) could be expected, and the free energy change at saturation would be reduced by $A_e \gamma_{lv}$. With the present system this probably occurs very near the saturation pressure.

On the basis of the previous discussion, the free energy changes due to adsorption on external and on internal surfaces were divided, at least to very near saturation, in Figure 10 by extending the linear portions of the plots corresponding to adsorption only on external surfaces to the saturation pressure. The difference between $A_e \Delta F$ and $A_i \Delta F$ gives the free energy change, $A_i \phi$, where A_i is the internal surface area per gram and ϕ is the expansion energy per cm^2 of internal surface and given by

$$\phi = \gamma_{sv} - \gamma_{so} + \Delta V \quad (6)$$

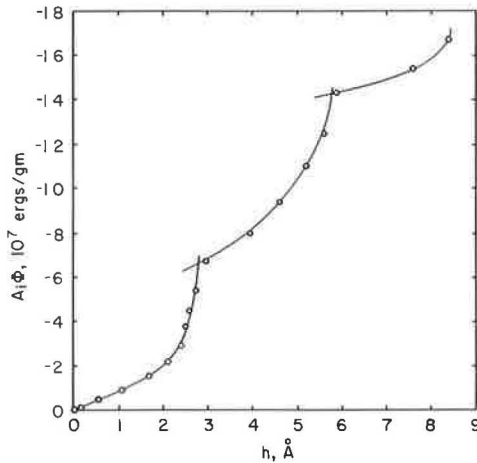


Figure 12. Plot of free energy change due to adsorption on, and separation of, internal surfaces vs interlayer separation, first adsorption run.

the clay surface. No new surfaces are formed nor do any disappear. The free energy change is due to extension of the film thickness and to expansion against the interaction forces. The free energy change due to extension of the film thickness is probably less than that for disappearance of solid surfaces and formation of solid-film interface; however, since the platelet separation is greater, the force of interaction is less and so the free energy change for formation of the second layer may be nearly the same as that for the first. The third layer of water may penetrate between the clay surface and existing interlayer water, but most probably enters between the first and second layer. Again, no new surfaces appear or disappear. The free energy change is due to extension of the film thickness and to expansion against forces of interaction further reduced by increased platelet separation. Since the free energy change on adsorption of the third layer is considerably less than that for the second, the change due to penetration between the first and second layers of water must be less than that for penetration between the clay surface and a water layer.

Swelling Pressures.—Roderick and Demirel (2), in an earlier study, suggested that there was a correlation between free energy data and swelling pressures exerted by montmorillonites. An estimate of the pressure required to prevent separation of clay platelets due to penetration of water between layers (or the swelling pressure exerted by the clay on uptake of interlayer water) was attempted using the basal spacing and free energy data of the present study.

At constant temperature, and assuming all work to be pressure-volume work, we have for free energy:

$$dF = Vdp \quad (7)$$

where V is the molar volume and p is the external pressure. For the present system, Eq. 7 becomes:

$$A_1 d\phi = Vdp$$

Assuming water is incompressible, the latter equation can be put into the following form:

$$d\phi = \frac{V}{A_1} dp = h_0 dp \quad (8)$$

where ΔV is the free energy change per cm^2 of internal surface due to separation of layers against the force of interaction.

Figure 12 plots $A_1\phi$ for the first adsorption run vs platelet separation, h . Values of $A_1\phi$ obtained from data of other runs produce very similar plots. The free energy change due to adsorption of the second molecular layer of interlayer water is as great as or slightly greater than that for adsorption of the first layer. The free energy change for formation of the third layer of interlayer water is substantially less than for the other two. The term, ϕ , for adsorption of the first layer of interlayer water is the free energy change due to disappearance of a solid surface and the formation of a solid-film interface, plus that due to separation against the force of interaction between platelets. The latter term will decrease the magnitude of the free energy change. The second layer of water must penetrate between the first and

where ϕ is the expansion energy (change in free energy due to adsorption on, and separation of, interlayer surfaces) per cm^2 ; V is the total volume of interlayer water at saturation pressure per gram of sodium montmorillonite; h_0 is the maximum platelet separation; and p is the applied pressure. From Eq. 8 we obtain

$$A_i \int_{\phi_S}^{\phi} d\phi = A_i \int_{p=0}^p h_0 dp \quad (9)$$

or

$$A_i \phi - A_i \phi_S = A_i h_0 p \quad (10)$$

or

$$p = \frac{A_i \phi - A_i \phi_S}{h_0 A_i} \quad (11)$$

where ϕ_S is the expansion energy when the clay is in equilibrium with saturated water vapor, p is the pressure required to prevent any platelet separation, and $p = 0$ is the pressure when the maximum separation is reached. The platelet separation is a function of ϕ as shown in Figure 12. The pressure required to prevent expansion beyond a certain separation h , when the sodium montmorillonite is in contact with saturated water vapor, may be obtained by determining the difference between $A_i \phi$ and $A_i \phi_S$ corresponding to separations h and h_0 , respectively, and dividing the difference by maximum separation h_0 . The results determined have the dimensions ergs/cm-gm, and must be divided by the internal surface area, A_i , to give the pressure in dynes/cm². Table 2 gives the external areas, A_e , determined for the first adsorption run by using various cross-sectional areas for the water molecule and the BET parameter q_m . Subtracting A_e from the total surface area of 748 m²/gm (from crystallographic data) gives the

TABLE 3

EXPANSION ENERGIES AND SWELLING PRESSURES DUE TO ADSORPTION OF WATER VAPOR ON INTERLAYER SURFACES OF SODIUM MONTMORILLONITE^a

Interlayer Water	Area Assigned to a Water Molecule (Å ²)	Internal Surface Area, A_i (m ² /gm)	Expansion Energy (ergs/cm ²)	Swelling Pressure, p (dynes/cm ²)	Swelling Pressure, p (tons/ft ²)
None present	10.8	665	—	300×10^6	313
	11.5	660	—	302×10^6	315
	17.5	614	—	325×10^6	339
One molecular layer	10.8	665	-9.8	181×10^6	190
	11.5	660	-9.8	184×10^6	192
	17.5	614	-10.6	197×10^6	206
Two molecular layers	10.8	665	-21.1	45×10^6	47
	11.5	660	-21.2	46×10^6	48
	17.5	614	-22.8	50×10^6	52
Three molecular layers	10.8	665	-24.8	—	—
	11.5	660	-25.0	—	—
	17.5	614	-26.9	—	—

^aFrom the separation indicated from the maximum separation.

internal surface area A_i per gram. The values of A_i for the various water molecular areas were determined and used to calculate the swelling pressures at various interlayer spacings. The results are indicated in Table 3. Also presented are values for the expansion energy, ϕ , obtained from Figure 12. The difference in the values obtained with various internal surface areas is probably less than the error due to the approximations of the methods for evaluation of the expansion energies and swelling pressures.

The expansion energy values at saturation may be due in part to capillary condensation in external pores. This would tend to make the values given when three molecular layers of water are present somewhat larger than the actual case. The expansion energies given for the adsorption of the first two layers of water are not affected by capillary condensation because it occurs near the saturation pressure.

Since the swelling pressures were obtained from the saturation point, any capillary condensation effects would tend to make the listed values somewhat larger than those due only to adsorption on internal surfaces. This may affect the values of swelling pressure when two layers of interlayer water are present to some degree, but would probably be negligible when compared with the large swelling pressures at lower interlayer water contents. Mielenz and King (36) reported swelling pressures from 2 to 11 tons/ft² for sodium montmorillonite in consolidometer tests. The present data suggest the pressures they obtained were due to hydration above two layers of interlayer water.

The swelling pressures given in Table 3 are those exerted when the sodium montmorillonite is in contact with saturated water vapor; the maximum observed interlayer separation is in equilibrium with the saturated vapor. If the sodium montmorillonite were in contact with liquid water, further expansion would occur and comparatively smaller swelling pressures might develop. In this region, for separation beyond three or four molecular layers of water, the surface hydration energies are no longer important and the smaller electrical double-layer forces become the major repulsive force between platelets (37). The further expansion exerting comparatively low additional pressure may be explained by attributing it to a low energy barrier (1).

CONCLUSIONS

The sorption isotherm data and X-ray diffraction data for water vapor adsorption and desorption by sodium montmorillonite, and data from the literature, indicate the following.

1. The change in average basal spacings of sodium montmorillonite takes place in a continuous but nonuniform manner with changes in relative pressure. Continuity is due to the simultaneous existence of varying numbers of molecular layers of interlayer water. Expansion occurs in three increments. Basal spacing and line width data show that average spacings correspond with an integral number of molecular layers of water just before each increment of expansion.
2. The relationship between relative humidity and the basal spacing of sodium montmorillonite is dependent on: (a) the source and method of preparation of the sample; (b) the initial conditions of the sample at the start of tests; and (c) whether data are collected during adsorption or desorption.
3. Basal spacing, line width, and free energy change data give evidence that the interlayer water builds up in a laminar manner.
4. Adsorption isotherms are more closely reproduced on successive adsorption-desorption runs than desorption isotherms.
5. The hysteresis displayed by the sorption isotherms is due in part to the formation of a thixotropic structure at high relative pressures, and in part to attractive interaction forces between sodium montmorillonite platelets.
6. X-ray diffraction data and BET plots indicate that the BET parameter, q_m , obtained reflects adsorption only on the external surfaces of the sodium montmorillonite. Apparently sodium montmorillonite prepared from Wyoming bentonite is unique in this respect.
7. The relationship between free energy changes and relative pressure and the X-ray diffraction data for the adsorption of water vapor by sodium montmorillonite allows sep-

aration of the free energy change into two components: one due to adsorption of the external surfaces, and one due to adsorption on, and separation of, the internal surfaces.

8. Free energy data and X-ray data show that the expansion energy (free energy change due to adsorption on, and separation of, internal surfaces) during formation of the second layer of interlayer water is approximately the same as that for formation of the first layer. The change during formation of the third layer is substantially less than those for the other two.

9. Free energy data and X-ray data permit the estimation of swelling pressures exerted by sodium montmorillonite due to the uptake of interlayer water when the material is in contact with saturated vapor. The swelling pressure exerted when the platelet separation is zero is about 325 tons/ft². The pressure exerted when one molecular layer of water separates clay platelets is about 200 tons/ft². The pressure exerted when two molecular layers of water separate platelets is about 50 tons/ft².

ACKNOWLEDGMENTS

The research reported herein was done at the Iowa Engineering Experiment Station, Iowa State University, under Project 505-S, Chemical Stabilization and Physico-Chemical Properties of Soils. This project was sponsored by the Iowa Highway Research Board under Project HR-97 and was supported with funds from the Iowa State Highway Commission and the U. S. Bureau of Public Roads.

REFERENCES

1. Demirel, T. Adsorption of Water Vapor by Sodium and Calcium Montmorillonite. Unpublished Ph.D. thesis, Iowa State Univ. of Sci. and Tech., 1962.
2. Roderick, G. L., and Demirel, T. Expansion of Montmorillonite Due to Adsorption of Water Vapor. *Iowa Acad. of Sci. Proc.* 70, pp. 280-289, 1963.
3. Brunauer, S. The Adsorption of Gases and Vapors. *Physical Adsorption*. Princeton, N. J., Princeton Univ. Press, 1943.
4. Klug, H. P., and Alexander, L. E. X-ray Diffraction Procedures for Polycrystalline and Amorphous Materials. New York, John Wiley and Sons, Inc., 1954.
5. Hendricks, S. B., and Jefferson, M. E. Structure of Kaolin and Talc-Pyrophyllite Hydrates and Their Bearing on Water Sorption of Clays. *American Mineralogist* Vol. 23, pp. 863-875, 1938.
6. Hendricks, S. B., Nelson, R. A., and Alexander, L. T. Hydration Mechanism of the Clay Mineral Montmorillonite Saturated with Various Cations. *American Chem. Soc. Jour.* Vol. 62, pp. 1457-1464, 1940.
7. MacEwan, D. M. C., Amil, A. R., and Brown, G. Interstratified Clay Minerals. In Brown, G., ed., *The X-ray Identification and Crystal Structures of Clay Minerals*. London, Mineralogical Soc., pp. 393-445, 1961.
8. Johns, W. D., Grim, R. E., and Bradley, W. F. Quantitative Estimations of Clay Minerals by Diffraction Methods. *Jour. of Sedimentary Petrology*, Vol. 24, pp. 242-251, 1954.
9. Milne, I. H., and Warshaw, C. M. Methods of Preparation and Control of Clay Mineral Specimens in X-ray Diffraction Analysis. *National Conf. on Clays and Clay Minerals*, Proc. 4, pp. 22-30, 1956.
10. Mooney, R. W., Keenan, A. G., and Wood, L. A. Adsorption of Water Vapor by Montmorillonite. II—Effect of Exchangeable Ions and Lattice Swelling as Measured by X-ray Diffraction. *Amer. Chemical Soc. Jour.* Vol. 74, pp. 1371-1374, 1952.
11. Gillery, G. H. Adsorption-Desorption Characteristics of Synthetic Montmorillonoids in Humid Atmospheres. *Amer. Mineralogist* Vol. 44, pp. 806-818, 1959.
12. Messina, M. L. Expansion of Fractional Montmorillonites Under Various Relative Humidities. *Clays and Clay Minerals*, Vol. 19, pp. 617-632, 1964.
13. Mooney, R. W., Keenan, A. G., and Wood, L. A. Adsorption of Water Vapor by Montmorillonite. I—Heat of Desorption and Application of BET Theory. *Amer. Chem. Soc. Jour.* 74, pp. 1367-1371, 1952.
14. Grim, R. E. *Clay Mineralogy*. New York, McGraw-Hill, 1953.

15. Winterkorn, H. F. The Science of Soil Stabilization. Highway Research Board Bull. 108, pp. 1-24, 1955.
16. Pauling, L. The Nature of the Chemical Bond. Ithaca, N. Y., Cornell Univ. Press, 1960.
17. Macey, H. H. Clay-Water Relationships and the Internal Mechanism of Drying. Ceramic Soc. Trans. 41, pp. 73-121, 1942.
18. Forslind, E. Crystal Structure and Water Adsorption of Clay Minerals. Swedish Cement and Concrete Res. Inst. Bull. 11, pp. 1-20, 1948.
19. Barshad, I. The Nature of Lattice Expansion and Its Relation to Hydration in Montmorillonite and Vermiculite. Amer. Mineralogist 34, pp. 675-684, 1949.
20. Brindley, G. W. X-ray Diffraction by Layer Lattices with Random Layer Displacements. In Brown, G., ed. The X-ray Identification and Crystal Structures of Clay Minerals, London, Mineralogical Soc., pp. 446-466, 1961.
21. McBain, J. W. An Explanation of Hysteresis in the Hydration and Dehydration of Gels. American Chem. Soc. Jour., Vol. 57, pp. 699-700, 1935.
22. Foster, A. G. The Sorption of Condensable Vapors by Porous Solids. I—The Applicability of the Capillary Theory. Faraday Soc. Trans. 28, pp. 645-657, 1932.
23. Barrer, R. M., and MacLeod, D. M. Intercalation and Sorption by Montmorillonite. Faraday Soc. Trans. 50, pp. 980-989, 1954.
24. Hirst, W. The Mechanical Interaction Between Mobile Insoluble Adsorbed Films, Capillary Condensed Liquid and Fine-Structured Solids. Faraday Soc. Discussions 3, pp. 22-28, 1948.
25. Johansen, R. T., and Dunning, H. N. Water-Vapor Adsorption on Clays. National Conf. on Clays and Clay Minerals, Proc. 6, pp. 249-258, 1959.
26. Brunauer, S., Emmett, P. H., and Teller, E. Adsorption of Gases in Multimolecular Layers. Amer. Chem. Soc. Jour. 60, pp. 309-319, 1938.
27. Adamson, A. W. Physical Chemistry of Surfaces. New York, Intersci. Pub., Inc, 1960.
28. Orchiston, H. D. Adsorption of Water Vapor. III—Homoionic Montmorillonites at 25°C. Soil Sci. 79, pp. 71-78, 1955.
29. Emmett, P. H., Brunauer, S., and Love, K. S. The Measurement of Surface Area of Soils and Soil Colloids by the Use of Low Temperature van der Waals Adsorption Isotherms. Soil Sci. 45, pp. 57-65, 1938.
30. Zettlemoyer, A. C., Young, G. J., and Chessick, J. J. Studies of the Surface Chemistry of Silicate Minerals. Jour. of Physical Chem., Vol. 59, pp. 962-966, 1955.
31. Clampitt, B. H., and German, D. E. Heat of Vaporization of Molecules at Liquid Vapor Interfaces. Jour. of Physical Chem., Vol. 62, pp. 438-440, 1958.
32. Takizawa, M. Mechanism of Water Vapor Adsorption on Bentonite. Tokyo Inst. of Physical and Chem. Res. Sci. Papers Vol. 54, pp. 313-322, 1960.
33. Bangham, D. H. The Gibbs Adsorption Equation and Adsorption on Solids. Faraday Soc. Trans. 33, pp. 805-811, 1937.
34. Fu, Y., and Bartell, F. E. Surface Area of Porous Adsorbents. Jour. of Physical and Colloid Chem. 55, pp. 662-675, 1951.
35. Jura, G., and Harkins, W. E. Determination of the Decrease of Free Surface Energy of a Solid by an Adsorbed Film. American Chem. Soc. Jour. 66, pp. 1356-1362, 1944.
36. Mielenz, R. C., and King, M. E. Physical-Chemical Properties and Engineering Performance of Clays. State of California Dept. of Natural Res., Div. of Mines Bull. 169, pp. 196-254, 1955.
37. van Olphen, H. An Introduction to Clay Colloid Chemistry. New York, Intersci. Publ., 1963.